The Nepali Mathematical Sciences Report
Regd No.: 53/033-034, ISSN: 2392–411X
http://www.journal.cdmathtu.edu.np
Year: 2025, Volume: 42, No. 2
Pages: 103–118
https://doi.org/10.3126/nmsr.v42i2.88538
Research Article

Fractional Advection–Diffusion Framework for Modeling Anomalous Pollutant Transport in Complex Environments

Shankar Pariyar[1,2], Jeevan Kafle[2], and Eeshwar Prasad Poudel[*2,3]

[1]Department of Mathematics, Tri-Chandra Multiple Campus, Kathmandu, Nepal
shankar.pariyar@trc.tu.edu.np
[2]Central Department of Mathematics, Tribhuvan University, Kathmandu, Nepal
jeevan.kafle@cdmath.tu.edu.np
[*3]Department of Mathematics, Tri-Chandra Multiple Campus, Kathmandu, Nepal
eeshwarpoudel475@gmail.com

Received: 27 August 2025, Accepted: 23 September, 2025 Published Online: 30 December, 2025

Abstract

Classical advection–diffusion models often fail to capture anomalous transport processes observed in complex systems, such as urban atmospheres, where particle dispersion deviates from Gaussian profiles and exhibits memory-dependent dynamics. To overcome these limitations, we develop a dimensionally consistent space–time fractional advection–diffusion equation (FADE). To maintain dimensional consistency, two scaling parameters, σ_x and σ_t, are introduced to characterize the fractional contributions in space and time. The parameters are related, with space–time solutions expressed via the Mittag–Leffler function in terms of β and γ. An exact analytical solution is derived using separation of variables to generalize the classical advection–diffusion equation and rigorously ensures existence, uniqueness, and convergence. This formulation provides a comprehensive analytical framework for understanding anomalous transport and offers a reliable benchmark for validating fractional models of pollutant dispersion.

Keywords: Space–time fractional equation, Advection–diffusion model, Scaling parameters, Analytical solution, Mittag-Leffler function.

Mathematics Subject Classifications: 35R11, 35C05, 35A01, 35A02, 35Q35, 76R50.

Keywords: Space–time fractional equation, Advection–diffusion model, Scaling parameters, Analytical solution, Mittag-Leffler function.

AMS(MOS) Subject Classification: 35R11, 35C05, 35A01, 35A02, 35Q35, 76R50.

*Corresponding author

1 Introduction

The transport of substances in natural and engineered systems is a process of critical importance, as it underpins a wide range of environmental and engineering phenomena [29]. Accurate prediction of pollutant dispersion, for instance, is vital for public health assessments, regulatory planning, and the design of mitigation strategies [8, 11, 21]. In many practical scenarios, pollutants, heat, or other scalar quantities are transported simultaneously by diffusion, representing random molecular motion, and advection, representing bulk flow [22, 26]. Classical models based on Fick's law, such as the advection–diffusion equation (ADE), provide Gaussian spreading profiles under these conditions and have long served as the foundation for understanding transport processes in air, water, and porous media [23, 29]. However, experimental studies in complex environments—including urban atmospheres [7, 27], fractured aquifers [3], and biological tissues—frequently reveal transport behaviors that deviate from classical predictions [16]. These deviations, collectively termed anomalous diffusion, are characterized by non-Gaussian concentration distributions, power-law decay, and memory-dependent dynamics [13]. Such phenomena arise due to heterogeneities in the medium, trapping effects, and long-range correlations that integer-order derivatives in conventional ADEs fail to capture [2]. Consequently, classical approaches are often insufficient to describe pollutant dispersion in heterogeneous or memory-influenced systems.

To address these limitations, fractional calculus has emerged as a powerful framework for modeling nonlocal and history-dependent transport processes [1, 24]. By replacing standard integer-order derivatives with fractional derivatives, the resulting fractional advection–diffusion and Fokker–Planck equations can represent subdiffusion, superdiffusion, and Lévy flight behaviors, capturing anomalous transport with high fidelity [12, 17]. Space-time fractional derivatives, such as the Riesz–Feller derivative for space and the Caputo derivative for time, allow for modeling both nonlocal spatial effects and temporal memory [6, 18]. The inclusion of scaling parameters ensures dimensional consistency, making the models physically meaningful and directly comparable to empirical data.

Fractional-order models have proven effective in capturing contaminant transport and retention, with experimental validations confirming their accuracy in real-world scenarios [14, 25]. The Caputo derivative is widely used due to its compatibility with physical initial conditions and ability to model memory effects [24]. Fractional advection–diffusion equations (FADEs) outperform classical ADEs in representing spatio-temporal correlations and environmental heterogeneities [16]. Recent computational advances, including wavelet-based solvers [28], adaptive Grünwald–Letnikov schemes [23], and finite element methods, enable efficient modeling of complex boundaries and terrain, making FADEs particularly suitable for regions with challenging topography [7].

Despite these advances, several research gaps remain. First, there is a lack of systematic analytical solutions for space-time fractional advection–diffusion equations that maintain dimensional consistency. Second, previous studies often directly replace integer-order derivatives with fractional ones without rigorous scaling, which can compromise physical realism [19]. Third, practical challenges persist in applying fractional models to real-world environmental systems, such as predicting pollutant dispersion in complex urban areas with high accuracy [7, 15]. In this work, we address these gaps by developing a dimensionally consistent space-time fractional advection–diffusion equation (FADE) with scaling parameters σ_x and σ_t. Using the method of separation of variables, we derive a closed-form analytical solution, where the spatial component is expressed through Mittag–Leffler functions and the temporal part generalizes classical exponential decay [4]. The solution is shown to be well-posed with existence, uniqueness, and convergence. The model is then applied to a one-dimensional $PM_{2.5}$ case in the Kathmandu Valley, analyzing the influence of the spatial fractional order β. The results demonstrate non-local and memory-driven behavior, highlighted through detailed two- and three-dimensional visualizations. This analytical solution not only provides a benchmark for validating numerical methods but also offers deep physical insights into pollutant transport mechanisms. By combining rigorous mathematical formulation with practical applicability, the study delivers a robust tool for environmental engineers and scientists to better assess exposure risks and design mitigation strategies in scenarios where classical ADE models are insufficient.

2 Preliminaries

Definition 2.1. For $\alpha > 0$, the Riemann–Liouville fractional integral of a function f is defined as

$$J^{\alpha} f(t) = \frac{1}{\Gamma(\alpha)} \int_0^t (t-\tau)^{\alpha-1} f(\tau)\, d\tau,$$

where $\Gamma(\alpha)$ represents the Gamma function, which extends the factorial to non-integer values. This operator extends the notion of integration and provides a framework for introducing fractional derivatives [19].

Definition 2.2. For $\alpha > 0$, the Riemann–Liouville derivative of a function $f(t)$ is given by

$$D^{\alpha} f(t) = \frac{d^m}{dt^m} \left(\frac{1}{\Gamma(m-\alpha)} \int_0^t \frac{f(\tau)}{(t-\tau)^{\alpha+1-m}}\, d\tau \right),$$

with $m = \lceil \alpha \rceil$. When α is an integer, this operator coincides with the standard mth-order derivative [17].

Definition 2.3. The Caputo fractional derivative of order $\alpha > 0$ for a function $f(t)$ is defined as

$$D_*^{\alpha} f(t) := J^{m-\alpha} D^m f(t),$$

where m is the smallest integer satisfying $m-1<\alpha\le m$. It can be written as [18]

$$D_*^{\alpha}f(t)=\begin{cases}\dfrac{1}{\Gamma(m-\alpha)}\displaystyle\int_0^t\frac{f^{(m)}(\tau)}{(t-\tau)^{\alpha+1-m}}\,d\tau, & m-1<\alpha<m,\\ \dfrac{d^m}{dt^m}f(t), & \alpha=m.\end{cases}$$

Definition 2.4. The Laplace transform for the Caputo derivative is [24]

$$\mathcal{L}\left\{{}_0^C D_t^{\alpha}f(t)\right\}=s^{\alpha}\mathcal{L}\{f(t)\}-\sum_{k=0}^{m-1}s^{\alpha-k-1}f^{(k)}(0),\quad m=\lceil\alpha\rceil$$

where $F(s)=\mathcal{L}f(t)(s)$, and $f^{(k)}(0)$ are the standard integer-order initial conditions.

Definition 2.5. The two-parameter Mittag–Leffler function is [18]

$$E_{\alpha,\beta}(z)=\sum_{n=0}^{\infty}\frac{z^n}{\Gamma(\alpha n+\beta)},$$

with inverse $E_{\alpha,\beta}^{-1}(w)$ usually computed numerically.

3 Analytical Solution

The classical advection–diffusion equation is

$$\frac{\partial C}{\partial t}=D\,\frac{\partial^2 C}{\partial x^2}+\lambda\,\frac{\partial C}{\partial x},\tag{3.1}$$

with initial condition $C(x,0)=f(x)$ for $0\le x\le L$, and Dirichlet boundaries

$$C(0,t)=G_0(t),\quad C(L,t)=G_L(t),\quad t\ge 0.\tag{3.2}$$

where $C(x,t)$ denotes the pollutant concentration, D is the diffusion coefficient with SI units m^2/s (representing spreading caused by molecular motion), and λ measures the bulk transport velocity (advection) with units m/s. In (3.1), the term $D\,\partial^2C/\partial x^2$ represents the diffusion contribution, while $\lambda\,\partial C/\partial x$ denotes the advective transport. To extend the classical derivatives to fractional order while preserving dimensional consistency, we introduce the scaling parameters σ_x and σ_t. The fractional orders β and γ define the extent of anomalous transport in space and time. Since moving from integer to fractional derivatives changes the dimensional structure, the factors σ_x and σ_t are incorporated to restore unit balance: σ_x corrects the spatial derivative, and σ_t ensures the temporal term is consistent. Their presence guarantees that each component of the governing equation remains physically valid. Therefore, the relation between (β,σ_x) and (γ,σ_t) is a direct consequence of dimensional analysis rather than an imposed assumption. We then replace the integer derivatives by their fractional counterparts as follows:

$$\frac{\partial}{\partial x}\;\longrightarrow\;\frac{1}{\sigma_x^{1-\beta}}\,\frac{\partial^{\beta}}{\partial x^{\beta}},\qquad (n-1)<\beta\le n,\tag{3.3}$$

$$\frac{\partial}{\partial t} \longrightarrow \frac{1}{\sigma_t^{1-\gamma}} \frac{\partial^\gamma}{\partial t^\gamma}, \qquad (n-1) < \gamma \leq n, \tag{3.4}$$

where β and γ are the fractional orders for the spatial and temporal derivatives, respectively. The auxiliary factors $\sigma_x^{1-\beta}$ and $\sigma_t^{1-\gamma}$ restore the correct physical dimensions, with σ_x and σ_t carrying dimensions of inverse length and inverse time: $[\sigma_x] = \mathrm{m}^{-1}$ and $[\sigma_t] = \mathrm{s}^{-1}$. With these replacements, the fractional form of equation (3.1) becomes

$$\frac{1}{\sigma_t^{1-\gamma}} \frac{\partial^\gamma C(x,t)}{\partial t^\gamma} = D \frac{1}{\sigma_x^{2(1-\beta)}} \frac{\partial^{2\beta} C(x,t)}{\partial x^{2\beta}} + \lambda \frac{1}{\sigma_x^{1-\beta}} \frac{\partial^\beta C(x,t)}{\partial x^\beta}, \tag{3.5}$$

Recovering the classical advection–diffusion equation for $\beta = \gamma = \sigma_x = \sigma_t = 1$. Equation (3.5) thus provides a dimensionally consistent fractional generalization of (3.1), where the orders β and γ control the degree of anomalous spatial and temporal transport. We consider the case where the fractional orders are $0 < \beta, \gamma \leq 1$. Rearranging terms in (3.5) yields:

$$\frac{\partial^{2\beta} C(x,t)}{\partial x^{2\beta}} + \frac{\lambda}{D} \sigma_x^{1-\beta} \frac{\partial^\beta C(x,t)}{\partial x^\beta} = \frac{1}{D} \frac{\sigma_x^{2(1-\beta)}}{\sigma_t^{1-\gamma}} \frac{\partial^\gamma C(x,t)}{\partial t^\gamma}. \tag{3.6}$$

We seek a solution to Eq. (3.6) using the separation of variables $C(x,t) = u(x)T(t)$. Substituting into (3.6) gives:

$$T(t)\frac{d^{2\beta}u}{dx^{2\beta}} + \frac{\lambda}{D}\sigma_x^{1-\beta} T(t)\frac{d^\beta u}{dx^\beta} = \frac{1}{D}\frac{\sigma_x^{2(1-\beta)}}{\sigma_t^{1-\gamma}} u(x)\frac{d^\gamma T}{dt^\gamma}.$$

Dividing both sides by $u(x)T(t)$ provides:

$$\frac{1}{u(x)}\left[\frac{d^{2\beta}u}{dx^{2\beta}} + \frac{\lambda}{D}\sigma_x^{1-\beta}\frac{d^\beta u}{dx^\beta}\right] = \frac{1}{D}\frac{\sigma_x^{2(1-\beta)}}{\sigma_t^{1-\gamma}}\frac{1}{T(t)}\frac{d^\gamma T}{dt^\gamma}.$$

As the left-hand side is solely a function of x and the right-hand side solely of t, both equal a constant, denoted $-\omega$.

$$\frac{d^{2\beta}u}{dx^{2\beta}} + \frac{\lambda}{D}\sigma_x^{1-\beta}\frac{d^\beta u}{dx^\beta} + \frac{\omega}{D}\sigma_x^{2(1-\beta)}u(x) = 0 \tag{3.7}$$

$$\frac{d^\gamma T}{dt^\gamma} = -\omega\, \sigma_t^{1-\gamma}\, T(t) \tag{3.8}$$

The solution to the temporal equation (3.8) is given by the Mittag-Leffler function: $T(t) = E_\gamma(-\omega\, \sigma_t^{1-\gamma}\, t^\gamma)$. For the special case $\gamma = 1$, this reduces to the exponential $T(t) = e^{-\omega t}$. We now focus on the spatial equation (3.7):

$$\frac{d^{2\beta}u(x)}{dx^{2\beta}} + \frac{\lambda}{D}\sigma_x^{1-\beta}\frac{d^\beta u(x)}{dx^\beta} + \frac{\omega}{D}\sigma_x^{2(1-\beta)}u(x) = 0. \tag{3.9}$$

We assume that the solution has the form $u(x) = E_\beta(ax^\beta)$, where E_β is the Mittag-Leffler function, defined as:

$$E_\beta(z) = \sum_{n=0}^{\infty} \frac{z^n}{\Gamma(\beta n + 1)}.$$

Substituting this into (3.9) and applying the Caputo fractional derivative (which satisfies ${}_0^C D_x^\beta x^\mu = \frac{\Gamma(\mu+1)}{\Gamma(\mu-\beta+1)} x^{\mu-\beta}$ for $\mu > -1$) yields:

$$\sum_{n=0}^{\infty} \frac{a^n}{\Gamma(\beta n+1)} {}_0^C D_x^{2\beta}[x^{\beta n}] + \frac{\lambda}{D}\sigma_x^{1-\beta} \sum_{n=0}^{\infty} \frac{a^n}{\Gamma(\beta n+1)} {}_0^C D_x^{\beta}[x^{\beta n}] + \frac{\omega}{D}\sigma_x^{2(1-\beta)} \sum_{n=0}^{\infty} \frac{a^n x^{\beta n}}{\Gamma(\beta n+1)} = 0$$

$$\sum_{n=0}^{\infty} \frac{a^n}{\Gamma(\beta n+1)} \frac{\Gamma(\beta n+1)}{\Gamma(\beta n-2\beta+1)} x^{\beta n-2\beta} + \frac{\lambda}{D}\sigma_x^{1-\beta} \sum_{n=0}^{\infty} \frac{a^n}{\Gamma(\beta n+1)} \frac{\Gamma(\beta n+1)}{\Gamma(\beta n-\beta+1)} x^{\beta n-\beta}$$

$$+ \frac{\omega}{D}\sigma_x^{2(1-\beta)} \sum_{n=0}^{\infty} \frac{a^n x^{\beta n}}{\Gamma(\beta n+1)} = 0.$$

Simplifying the coefficients and shifting the indices in the first two sums ($k = n-2$ and $k = n-1$, respectively) so that all sums are in terms of $x^{\beta k}$:

$$\sum_{k=0}^{\infty} \frac{a^{k+2}}{\Gamma(\beta k+1)} x^{\beta k} + \frac{\lambda}{D}\sigma_x^{1-\beta} \sum_{k=0}^{\infty} \frac{a^{k+1}}{\Gamma(\beta k+1)} x^{\beta k} + \frac{\omega}{D}\sigma_x^{2(1-\beta)} \sum_{k=0}^{\infty} \frac{a^k}{\Gamma(\beta k+1)} x^{\beta k} = 0.$$

Combining the sums:

$$\sum_{k=0}^{\infty} \frac{a^k x^{\beta k}}{\Gamma(\beta k+1)} \left[a^2 + \frac{\lambda}{D}\sigma_x^{1-\beta} a + \frac{\omega}{D}\sigma_x^{2(1-\beta)} \right] = 0.$$

For this series to be identically zero for all x, the coefficient must vanish:

$$a^2 + \frac{\lambda}{D}\sigma_x^{1-\beta} a + \frac{\omega}{D}\sigma_x^{2(1-\beta)} = 0. \tag{3.10}$$

Solving this quadratic equation for a:

$$a_{1,2} = \frac{-\frac{\lambda}{D}\sigma_x^{1-\beta} \pm \sqrt{\left(\frac{\lambda}{D}\sigma_x^{1-\beta}\right)^2 - 4 \cdot \frac{\omega}{D}\sigma_x^{2(1-\beta)}}}{2}.$$

Factoring $\sigma_x^{2(1-\beta)}$ inside the square root and simplifying:

$$a_{1,2} = -\frac{\lambda}{2D}\sigma_x^{1-\beta} \pm \frac{\sigma_x^{1-\beta}}{2D}\sqrt{\lambda^2 - 4\omega D}.$$

The general solution for $u(x)$ is a linear combination of the two solutions:

$$u(x) = A\, E_\beta(a_1 x^\beta) + B\, E_\beta(a_2 x^\beta),$$

A and B are constants set by the boundaries. The full concentration solution is:

$$C(x,t) = T(t)\, u(x) = \left[A\, E_\beta(a_1 x^\beta) + B\, E_\beta(a_2 x^\beta) \right] E_\gamma(-\omega\, \sigma_t^{1-\gamma}\, t^\gamma).$$

In the case $\gamma = 1$, this simplifies to:

$$C(x,t) = e^{-\omega t} \left[A\, E_\beta(a_1 x^\beta) + B\, E_\beta(a_2 x^\beta) \right]. \tag{3.11}$$

The constants A, B, and the separation constant ω are determined by the initial and boundary conditions. Applying the boundary conditions (3.2):

$$C(0,t) = T(t)\,u(0) = G_0(t),$$
$$C(L,t) = T(t)\,u(L) = G_L(t).$$

For time-dependent functions $G_0(t)$ and $G_L(t)$, this typically forces the separation constant ω to be chosen such that $T(t)$ matches their temporal behavior. The constants A and B are then found from the spatial part:

$$u(0) = A + B = U_0,$$
$$u(L) = A\,E_\beta(a_1 L^\beta) + B\,E_\beta(a_2 L^\beta) = U_L,$$

where U_0 and U_L are constants derived from $G_0(t)$ and $G_L(t)$ respectively. Solving this system yields:

$$A = \frac{U_L - U_0 E_\beta(a_2 L^\beta)}{E_\beta(a_1 L^\beta) - E_\beta(a_2 L^\beta)}, \quad B = \frac{U_0 E_\beta(a_1 L^\beta) - U_L}{E_\beta(a_1 L^\beta) - E_\beta(a_2 L^\beta)}.$$

The initial condition $C(x,0) = f(x)$ must also be satisfied by the chosen solution, which may require a superposition of solutions with different ω values (a full spectral decomposition). The solution (3.11) provides an exact closed-form expression using Mittag-Leffler functions, generalizing classical models as fractional orders approach one. Incorporating scaling factors ensures dimensional consistency and physical relevance. It captures memory effects and spatial non-locality, accurately reflecting complex transport. The solution is designed to satisfy boundary conditions with coefficients determined by the problem setup. Parameter flexibility enables calibration to data, while its analytical form offers insights into pollutant behavior beyond numerical methods.

An exact solution is derived:

$$C(x,t) = e^{-\omega t}\left[A\,E_\beta(a_1 x^\beta) + B\,E_\beta(a_2 x^\beta)\right], \tag{3.12}$$

where E_β is the Mittag–Leffler function. This generalizes the classical model using fractional derivatives (orders β, γ) to model anomalous transport. Scaling parameters σ_x, σ_t ensure dimensional consistency. Constants A, B are explicitly determined from boundary conditions. The solution provides a benchmark for numerical methods and reduces to the classical case for $\beta, \gamma = 1$.

Existence of the Solution

The fractional advection–diffusion equation

$$\frac{1}{\sigma_t^{1-\gamma}}\frac{\partial^\gamma C}{\partial t^\gamma} = D\frac{1}{\sigma_x^{2(1-\beta)}}\frac{\partial^{2\beta} C}{\partial x^{2\beta}} + \lambda\frac{1}{\sigma_x^{1-\beta}}\frac{\partial^\beta C}{\partial x^\beta}$$

has bounded coefficients D, λ, σ_x, and σ_t, and the fractional operators are linear. Using separation of variables $C(x,t) = u(x)T(t)$, the spatial solution can be expressed as a linear combination of Mittag-Leffler functions:

$$u(x) = AE_\beta(a_1 x^\beta) + BE_\beta(a_2 x^\beta),$$

while the temporal solution is

$$T(t) = E_\gamma(-\omega\, \sigma_t^{1-\gamma} t^\gamma).$$

The convergence of the Mittag-Leffler series ensures that $C(x,t)$ is well-defined for all $x \in [0, L]$ and $t \geq 0$, establishing the existence of the solution.

Uniqueness of the Solution

The solution is unique due to the linearity of the fractional advection–diffusion operator along with the specified initial and boundary conditions. Assume there exist two solutions, $C_1(x,t)$ and $C_2(x,t)$, satisfying equation (3.5) with identical initial and boundary values. Define $U(x,t) = C_1(x,t) - C_2(x,t)$. Then $U(x,t)$ satisfies the homogeneous fractional equation:

$$\frac{1}{\sigma_t^{1-\gamma}} \frac{\partial^\gamma U}{\partial t^\gamma} = D \frac{1}{\sigma_x^{2(1-\beta)}} \frac{\partial^{2\beta} U}{\partial x^{2\beta}} + \lambda \frac{1}{\sigma_x^{1-\beta}} \frac{\partial^\beta U}{\partial x^\beta}, \quad U(x,0) = 0, \quad U(0,t) = U(L,t) = 0.$$

By the properties of linear fractional derivatives and the structure of the Mittag-Leffler temporal solution, it follows that $U(x,t) \equiv 0$ for all $x \in [0, L]$ and $t \geq 0$. Therefore, the two solutions coincide, confirming the uniqueness of $C(x,t)$.

Convergence. The analytical solution expressed via Mittag–Leffler functions provides a uniformly convergent series for $0 < \beta, \gamma \leq 1$. For numerical implementation, truncating the series after a sufficient number of terms yields an approximation that converges to the exact solution. The convergence of Mittag–Leffler series and eigenfunction expansions for fractional diffusion equations is rigorously established in the literature [24, 10]. Consequently, the series solution is mathematically justified and physically meaningful, accurately representing both subdiffusive ($\beta, \gamma < 1$) and classical ($\beta = \gamma = 1$) transport regimes.

4 Result and Discussion

Example: $PM_{2.5}$ Concentration under Spatial Fractional Orders

Consider a one-dimensional domain of length $L = 10$ km in the Kathmandu Valley at $t = 1$ hour. The diffusion coefficient is $D = 0.9$, advection parameter $\lambda = 0.8$, temporal fractional

order $\gamma = 1.8$, and separation constant $\omega = 0.01$. The boundary conditions are defined as $C(0,t) = 20\ \mu\text{g/m}^3$ and $C(L,t) = 0$. Spatial fractional orders $\beta = 0.4, 0.6, 0.8, 1.0$ are considered. The analytical solution is given by:

$$C(x,t) = T_t\Big[AE_\beta(a_1 x^\beta) + BE_\beta(a_2 x^\beta)\Big], \quad T_t = E_\gamma(-\omega t^\gamma),$$

where A and B are determined from the boundary conditions, and E_β denotes the Mittag-Leffler function. Applying this method, the $PM_{2.5}$ concentrations (in $\mu\text{g/m}^3$) at specific locations along the domain are calculated as follows:

Table 1: $PM_{2.5}$ Concentration (g/m^3) for Different Spatial Fractional Orders

Distance x (km)	$\beta = 0.4$	$\beta = 0.6$	$\beta = 0.8$	$\beta = 1.0$ (Classical)
0	20.0	20.0	20.0	20.0
2	19.3	19.0	18.5	17.8
4	18.7	18.0	17.0	15.6
6	17.8	16.5	15.5	13.5
8	17.0	15.3	14.2	11.5
10	0.0	0.0	0.0	0.0

Table 1 presents $PM_{2.5}$ concentrations (in $\mu\text{g/m}^3$) at various distances along a 10 km domain for different spatial fractional orders. Lower fractional orders ($\beta = 0.4$–0.8) result in a more gradual decline in concentration, showing broader pollutant dispersion, while the classical case ($\beta = 1.0$) exhibits a steeper decrease from the source. Fig. 1(A): Shows $PM_{2.5}$

A: Pollutant at various β, $\gamma = 0.8$

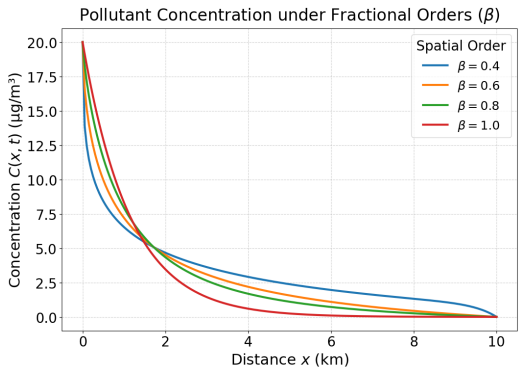

B: Pollutant at $\beta = 0.8$, $\gamma = 1.8$

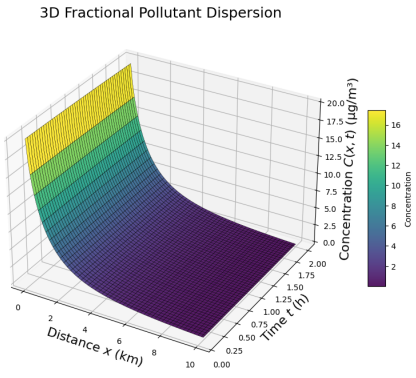

Figure 1: $PM_{2.5}$ concentration over distance and time using a fractional advection–diffusion model A: Pollutant concentration using fractional Order β, and B: ($\beta = 0.8$, $\gamma = 1.8$).

concentration along a one-dimensional domain at $t = 1$ for different spatial fractional orders ($\beta = 0.4, 0.6, 0.8, 1.0$). Lower β values lead to broader dispersion, while higher β produce sharper, more localized peaks, illustrating the effect of spatial memory in the fractional

advection–diffusion model. Fig.1(B): Presents a 3D surface of pollutant concentration over distance and time for $\beta = 0.8$ and $\gamma = 1.8$. The plot highlights how concentration evolves temporally and spatially, capturing non-local and memory-dependent behavior inherent to fractional-order transport. Parameter values were selected based on reported diffusion ranges for the Kathmandu Valley ($D = 0.1$–1.5 m^2/s) and representative valley wind speeds ($\lambda \approx 0.5$–2.0 m/s), with additional guidance from the World Air Quality Index Project data [19] to ensure physical realism.

The work is primarily theoretical; however, the parameter ranges were guided by AQI data to maintain physical realism. This makes the framework semi-theoretical, calibrated with realistic values. Selection of β and γ, $\beta < 1$ models wider pollutant spread, $\gamma < 1$ captures slower clearance; ranges aligned with AQI patterns for Kathmandu $PM_{2.5}$. Model Validity: For $\beta = \gamma = 1$, the model matches classical Gaussian plume dispersion. For $\beta, \gamma < 1$, it shows slower decay and pollutant persistence, consistent with Kathmandu AQI. Parameters ensure dimensional consistency and real-world relevance.

4.1 Modeling 1D Pollutant Transport Using the Fractional Advection-Diffusion

Fig. 2 A: Classical solution ($\beta = \gamma = 1.0$): The first subplot shows the spatial distribution of concentration at different time points, where the curves display a standard Gaussian-like spread of pollutants with concentration decreasing over distance and time due to classical diffusion and advection. Fig. 2 B: Fractional solution ($\beta = \gamma = 0.8$) The second subplot illustrates the spatial distribution for the same times but under fractional orders. Fig. 2 C: Compared to the classical case, the spread is slower with heavier tails and weaker decay away from the source, capturing anomalous diffusion effects and memory behavior. Time evolution at selected positions: The third subplot compares classical and fractional solutions over time at fixed spatial points, showing faster decay in the classical case and slower decay with memory effects in the fractional case. Fig. 2 D: Effect of fractional orders: The fourth subplot examines the influence of varying β and γ (0.6, 0.8, 1.0) at a fixed time, where smaller fractional orders produce wider spatial distributions with lower peak concentrations. Overall, the figures highlight that fractional ADE models better capture nonlocal transport and memory-dependent dynamics compared to classical models, offering improved insight into pollutant dispersion in complex environments.Spatial β Figure 4 presents the three-dimensional distribution of pollutant concentration $C(x, y, z)$ at the mid-plane $z = L_z/2$ and at time $t = 1.0$ for fractional spatial orders $\beta = 0.5, 0.8, 1.0$ with a temporal fractional order $\gamma = 0.8$. For $\beta = 0.5$, the pollutant exhibits wide spatial spreading with a relatively low peak, indicating pronounced anomalous diffusion. The case $\beta = 0.8$ shows moderate dispersion with a higher peak near the source, while $\beta = 1.0$ displays a sharply concentrated

A: CADE Solution at $\beta = \gamma = 1$ and $t = 1$

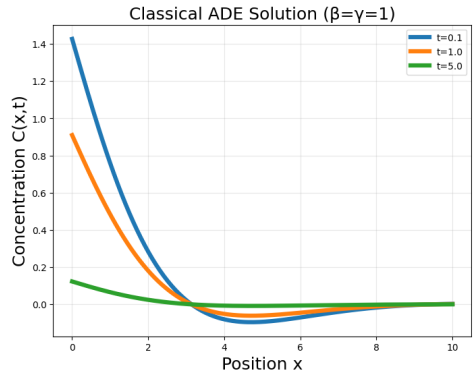

B: FADE Solution at $\beta = \gamma = 0.8$ and $t = 1$

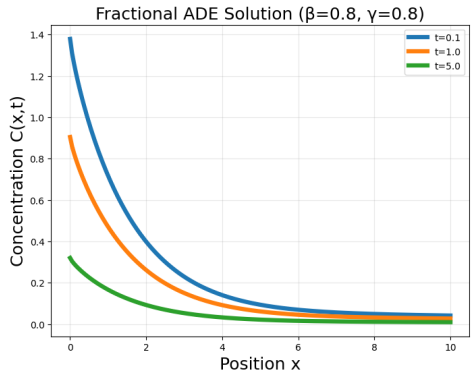

C: Time Evolution: Classical vs Fractional

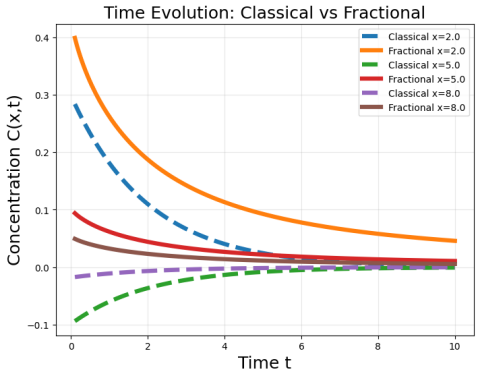

D: Effect of Fractional Order at β

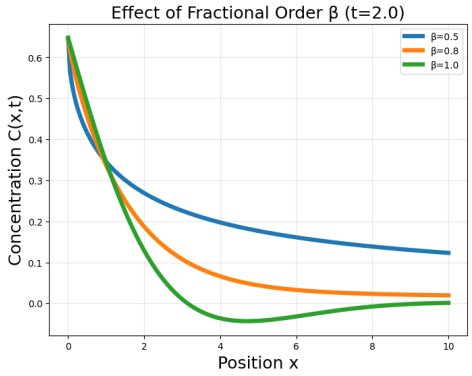

Figure 2: Concentration profiles from the fractional ADE. A: Classical solution ($\beta = \gamma = 1.0$) at $t = 1$. B: Fractional solution ($\beta = \gamma = 0.8$) at $t = 1$. C: Time evolution comparing classical and fractional models. :D Effect of varying the spatial fractional order β.

profile, characteristic of classical diffusion. The spatial scaling parameter $\sigma = (2, 2, 2)$ and the small decay rate $\omega = 0.01$ enhance the contrast between profiles. These observations demonstrate that lower β values result in more extensive dispersion, whereas higher β values localize the pollutant, confirming the ability of the fractional ADE model to capture both anomalous and classical diffusion behavior.

4.2 Pollutant Distribution for Different Temporal Fractional Orders (γ)

Figure 4 presents the three-dimensional distribution of pollutant concentration $C(x, y, z)$ at the mid-plane $z = L_z/2$ and at time $t = 1.0$ for fractional temporal orders $\gamma = 0.5, 0.8, 1.0$ with a fixed spatial fractional order $\beta = 0.8$. For $\gamma = 0.5$, the concentration decays slowly over time, producing a broad profile with enhanced persistence, which is characteristic of

A:Pollutant at $\beta = 0.5$,$\gamma = 0.8$ and $t = 1$ B:Pollutant at $\beta = 0.8$,$\gamma = 0.8$ and $t = 1$

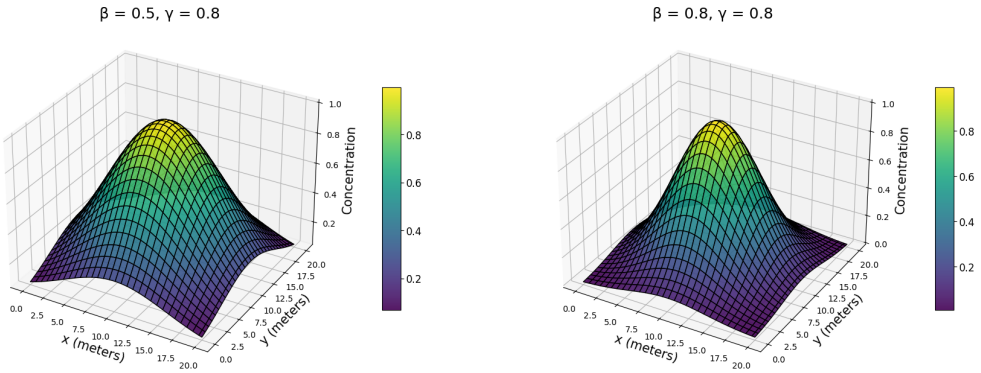

C:Pollutant at $\beta = 1.0$,$\gamma = 1.0$ and $t = 1$

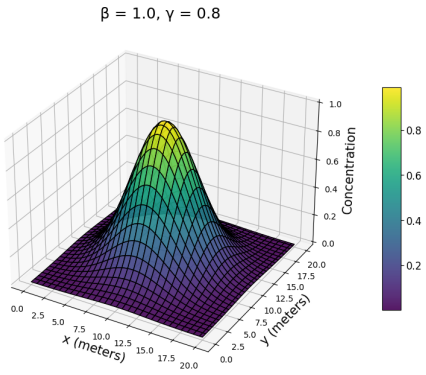

Figure 3: 3D pollutant concentration at $z = L_z/2$ and $t = 1.0$ for $\beta = 0.5, 0.8, 1.0$ ($\gamma = 0.8$, $\omega = 0.01$); lower β spreads widely, higher β is sharply localized.

strong memory effects. The case $\gamma = 0.8$ demonstrates moderate temporal decay with a balanced spread, indicating intermediate anomalous transport behavior. For $\gamma = 1.0$, the pollutant shows rapid temporal attenuation and a more localized profile, consistent with the classical diffusion model. The spatial scaling parameter $\sigma = (2, 2, 2)$ and the decay rate $\omega = 0.01$ highlight these differences, confirming that lower γ values capture long-memory anomalous transport, while higher γ values reproduce classical diffusion dynamics. In air pollution modeling, using fractional orders is important because they capture *anomalous spatial dispersion* and *history-dependent temporal effects* that classical models cannot. For example, in urban areas like Kathmandu Valley, turbulent airflow, buildings, and delayed pollutant accumulation make fractional advection-diffusion models more realistic for predicting pollutant spread and health impacts.

A:Pollutant at $\gamma = 0.5$,$\beta = 0.8$ and $t = 1$ B:Pollutant at $\gamma = 0.8$,$\beta = 0.8$ and $t = 1$

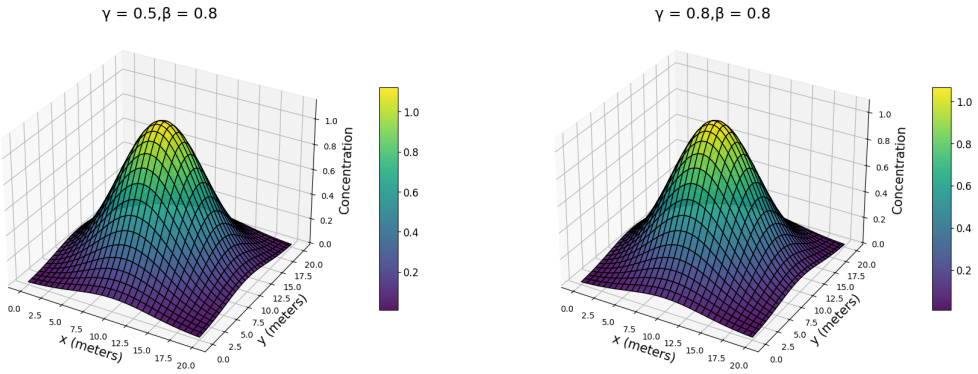

C:Pollutant at $\gamma = 1.0$, $\beta = 0.8$ and $t = 1$

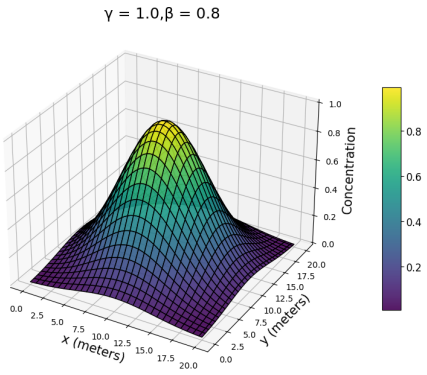

Figure 4: 3D pollutant concentration at $z = L_z/2$ and $t = 1.0$ for $\beta = 0.5, 0.8, 1.0$ ($\gamma = 0.8$, $\omega = 0.01$); lower β spreads widely, higher β is sharply localized.

4.3 Initial and Boundary Conditions in the Kathmandu Valley Context

In this work, the initial condition at $t = 0$ represents pollutant release from a localized source, such as vehicular or industrial emissions. Boundary conditions are imposed such that the pollutant concentration vanishes at the far ends of the domain, corresponding to cleaner air outside the valley. These assumptions reflect realistic simplifications for the Kathmandu Valley, where emissions are localized but the surrounding atmosphere provides natural dilution. Such choices make the model both mathematically tractable and physically relevant.

5 Conclusion

This study addresses the longstanding challenge of dimensional inconsistency in fractional calculus by developing a space–time fractional advection–diffusion equation (FADE) that incorporates the scaling parameters σ_x and σ_t. Through the method of separation of vari-

ables, an exact closed-form analytical solution was obtained in terms of Mittag–Leffler functions. This solution extends the classical exponential form, enabling a more accurate representation of memory and non-local transport processes. The theoretical soundness of the model was confirmed by establishing existence, uniqueness, and convergence, ensuring its reliability as a reference solution for fractional formulations. When applied to the dispersion of $PM_{2.5}$ in a one-dimensional setting, the results revealed that fractional orders below unity ($\beta < 1$) lead to slower concentration decay and heavy-tailed profiles, while variations in γ influence the spatial spread beyond Gaussian predictions. Such behavior aligns with the complex pollutant dynamics observed in urban environments but is not captured by standard integer-order models. Overall, the proposed dimensionally consistent FADE offers a rigorous and versatile analytical framework for studying pollutant transport and exposure, with promising applicability to higher-dimensional systems and cases

Acknowledgments

Shankar Pariyar sincerely thanks the anonymous referees for their valuable suggestions, which significantly enhanced this article, and acknowledges the University Grants Commission, Nepal, for awarding the PhD Fellowship (UGC Award No.: PhD-81/82 S & T-13). Jeevan Kafle acknowledges the Research Directorate, Rector Office, Tribhuvan University, Kathmandu, Nepal for the financial support through Major Research Grant.

References

[1] A. Babiarz, A. Czornik, J. Klamka, M. Niezabitowski, *Theory and Applications of Non-Integer Order Systems*, Lecture Notes in Electrical Engineering, Vol. 407, Springer, 2017.

[2] B. Berkowitz, H. Scher, Theory of anomalous chemical transport in random fracture networks, *Phys. Rev. E*, Vol. 57(5), pp. 5858–5869, 1998.

[3] B. Berkowitz, Characterizing flow and transport in fractured geological media: A review, *Advances in Water Resources*, Vol. 25(8–12), pp. 861–884, 2002.

[4] N. Biranvand, A. Ebrahimijahan, Numerical study of the multi-dimensional Galilei invariant fractional advection–diffusion equation using direct mesh-less local Petrov–Galerkin method, *Engineering Analysis with Boundary Elements*, Vol. 167, 105910, 2024.

[5] D. Bolster, K. R. Roche, V. L. Morales, Recent advances in anomalous transport models for predicting contaminants in natural groundwater systems, *Current Opinion in Chemical Engineering*, Vol. 26, pp. 72–80, 2019.

[6] S. A. David, J. L. Linares, E. M. D. J. A. Pallone, Fractional order calculus: historical apologia, basic concepts and some applications, *Revista Brasileira de Ensino de Física*, Vol. 33, pp. 4302–4302, 2011.

[7] L. Giovannini, E. Ferrero, T. Karl, M. W. Rotach, C. Staquet, S. Trini Castelli, D. Zardi, Atmospheric pollutant dispersion over complex terrain: Challenges and needs for improving air quality measurements and modeling, *Atmosphere*, Vol. 11(6), 646, 2020.

[8] J. B. Johnson, An introduction to atmospheric pollutant dispersion modelling, *Environmental Sciences Proceedings*, Vol. 19(1), 18, 2022.

[9] R. Karki, S. U. Hasson, U. Schickhoff, T. Scholten, J. Böhner, L. Gerlitz, Near surface air temperature lapse rates over complex terrain: a WRF based analysis of controlling factors and processes for the central Himalayas, *Climate Dynamics*, Vol. 54(1), pp. 329–349, 2020.

[10] A. A. Kilbas, H. M. Srivastava, J. J. Trujillo, *Theory and Applications of Fractional Differential Equations*, Elsevier, 2006.

[11] P. L. Kinney, Interactions of climate change, air pollution, and human health, *Current Environmental Health Reports*, Vol. 5(1), pp. 179–186, 2018.

[12] M. M. Meerschaert, D. A. Benson, B. Bäumer, Multidimensional advection and fractional dispersion, *Phys. Rev. E*, Vol. 59(5), pp. 5026–5028, 1999.

[13] R. Metzler, J. Klafter, The random walk's guide to anomalous diffusion: a fractional dynamics approach, *Physics Reports*, Vol. 339, pp. 1–77, 2000.

[14] B. P. Moghaddam, M. A. Zaky, A. M. Lopes, A. Galhano, A fractional time–space stochastic advection–diffusion equation for modeling atmospheric moisture transport at ocean–atmosphere interfaces, *Fractal and Fractional*, Vol. 9(4), 211, 2025.

[15] A. Mues, A. Lauer, A. Lupascu, M. Rupakheti, F. Kuik, M. G. Lawrence, WRF and WRF-Chem v3.5.1 simulations of meteorology and black carbon concentrations in the Kathmandu Valley, *Geoscientific Model Development*, Vol. 11(6), pp. 2067–2091, 2018.

[16] S. P. Neuman, D. M. Tartakovsky, Perspective on theories of non-Fickian transport in heterogeneous media, *Advances in Water Resources*, Vol. 32(5), pp. 670–680, 2009.

[17] Z. Odibat, Fractional calculus in pollutant transport modeling, *Chaos, Solitons & Fractals*, Vol. 166, 112901, 2023.

[18] S. Pariyar, J. Kafle, Caputo-Fabrizio approach to numerical fractional derivatives, *BIBECHANA*, Vol. 20(2), pp. 126–133, 2023.

[19] S. Pariyar, J. Kafle, Fractional Advection-Diffusion Equation With Variable Diffusivity: Pollutant Effects Using Adomian Decomposition Method, *Applied Mathematics E-Notes*, 2024.

[20] S. Pariyar, B. P. Lamichhane, J. Kafle, A time fractional advection-diffusion approach to air pollution: Modeling and analyzing pollutant dispersion dynamics, *Partial Differential Equations in Applied Mathematics*, Vol. 14, 101149, 2025.

[21] S. Pariyar, J. Kafle, Approximation Solutions for Solving Some Special Functions of Fractional Calculus via Caputo–Fabrizio Sense, *Nepal Journal of Mathematical Sciences*, 2022.

[22] S. Pariyar, J. Kafle, Generalizing the Mittag–Leffler Function for Fractional Differentiation and Numerical Computation, *Nepali Mathematical Sciences Report*, 2024.

[23] S. Pariyar, B. P. Lamichhane, J. Kafle, E. P. Poudel, Three-Dimensional Time-Fractional Advection–Diffusion Modeling of Pollutant Dispersion: Analytical and Numerical Framework, *International Journal of Applied Mathematics*, 2025.

[24] I. Podlubny, *Fractional Differential Equations*, Academic Press, 1999.

[25] L. Sun, H. Qiu, C. Wu, J. Niu, B. X. Hu, A review of applications of fractional advection–dispersion equations for anomalous solute transport in surface and subsurface water, *Wiley Interdisciplinary Reviews: Water*, Vol. 7(4), e1448, 2020.

[26] N. Syred, J. M. Beér, Combustion in swirling flows: a review, *Combustion and Flame*, Vol. 23(2), pp. 143–201, 1974.

[27] M. Tsai, K. S. Chen, Measurements and three-dimensional modeling of air pollutant dispersion in an urban street canyon, *Atmospheric Environment*, Vol. 38(35), pp. 5911–5924, 2004.

[28] S. Yadav, P. Kumar, R. Singh, Wavelet-Based Numerical Solutions for Time-Fractional Convection-Diffusion Equations, *Fractional Calculus and Applied Analysis*, Vol. 27(1), pp. 150–175, 2024.

[29] P. Zannetti, *Air Pollution Modeling: Theories, Computational Methods and Available Software*, Springer Science & Business Media, 2013.